International Journal of Thermophysics, Vol. 28, No. 2, April 2007 (© 2007)
DOI: 10.1007/s10765-007-0181-3

Corresponding-States Analysis of the Surface Tension of Simple, Polar, and Ionic Fluids

V. C. Weiss[1,2,3] and W. Schröer[4]

The liquid–vapor interfacial tension of various simple, polar, and ionic fluids is studied in a corresponding-states analysis that was originally suggested by Guggenheim. Data for real fluids are compared to results of simulations and theoretical predictions for model fluids of each of the three types (namely, the Yukawa fluid, the square-well fluid, a fluid consisting of dipolar hard spheres, and the restricted primitive model of ionic fluids). As already demonstrated by Guggenheim, the data for simple and weakly polar fluids map onto a master curve. Strongly dipolar, associating fluids, which may also exhibit hydrogen-bonding (e.g., water), show deviations from this master curve at low temperatures. In addition, the surface tension of these fluids shows a characteristic sigmoid behavior as a function of temperature. A similar behavior is found from simulations of the ionic model fluid, but not from the electrolyte theories available up to now, for which we present new results here. Exceptionally low values of the reduced surface tension are obtained for hydrogen fluoride and for the Onsager model of dipolar fluids, which, however, agree remarkably well with each other in a corresponding-states plot.

KEY WORDS: corresponding states; interfaces; model fluids; surface tension.

1. INTRODUCTION

Since the days of van der Waals, the concept of corresponding states has proved useful in identifying universalities in the behavior of fluids by

[1] School of Engineering and Science, International University Bremen, P.O. Box 750561, 28725 Bremen, Germany.
[2] Present address: Eduard-Zintl-Institut für Anorganische und Physikalische Chemie, Technische Universität Darmstadt, Petersenstrasse 20, 64287 Darmstadt, Germany.
[3] To whom correspondence should be addressed. E-mail: v.weiss@theo.chemie.tu-darmstadt.de
[4] Institut für Anorganische und Physikalische Chemie, Universität Bremen, 28359 Bremen, Germany.

scaling out the characteristic differences of the individual substances. The concept was revived and further developed by Guggenheim [1], who suggested that the surface tension γ should be a universal function of the reduced temperature T/T_c, where T_c denotes the critical temperature, for all simple fluids, if it was scaled according to

$$\gamma_{red}(T/T_c) = \frac{\gamma(T)}{\rho_c^{2/3} k T_c}, \tag{1}$$

where ρ_c is the critical density and k denotes Boltzmann's constant. This particular type of scaling is motivated by the desire to account for the different strengths of intermolecular interactions by dividing by T_c, while different densities of molecules at the liquid–vapor interface are accounted for by the fractional power of 2/3 of the critical density ρ_c of the respective fluid. Guggenheim demonstrated the validity of the concept for noble gases [1]. In the same paper, he noted that deviations from the so-obtained master curve for simple fluids should not be regarded as "failures" of the corresponding-states principle, but rather as providing us with interesting additional information on fluids that do not adhere to the universal scaling of simple fluids.

The law of corresponding states can be shown to apply to families of underlying interaction potentials that can be characterized by only two parameters [2]. A famous example of such a potential is the Lennard-Jones potential which proved useful in describing the properties of simple fluids, such as noble gases. In terms of studying deviations from the master curve for simple fluids, three-parameter potentials obeying spherical symmetry are the simplest type of interaction that may be of interest. Additionally, two-parameter potentials which show strong anisotropy, such as dipolar interactions, or which are of significantly longer range than the usual van der Waals dispersion interactions, such as the Coulombic interaction between ions, are expected to give rise to a behavior that differs from that of simple fluids.

In this paper, we will compare the surface-tension (liquid–vapor interfacial tension, to be more precise) data for simple fluids described by three-parameter potentials for different ranges of the interactions, for polar fluids, and for ionic fluids. Wherever possible, experimental data for real fluids will be shown together with the results for model fluids obtained from computer simulations and from (simple) theories. One of the great advantages of the corresponding-states approach is that the data for real and model fluids can be compared directly, without the need for assumptions on the actual size of molecules because all data are scaled by the critical parameters of the respective fluid.

The methodology of calculating the surface tension of model fluids is reviewed briefly in Section 2. In Section 3, simple fluids having spherically symmetrical interaction potentials of variable range are considered; for computational simplicity and availability of simulation results, we study the Yukawa fluid in Section 3.1 and the square-well fluid in Section 3.2. Polar fluids are the subject of Section 4, in which we will compare the behavior of various strongly polar fluids to the results we obtained for the model of dipolar hard spheres within Onsager theory [3]. Experimental results for ionic systems (molten salts) are rare; the few data available are compared to simulation results and theoretical predictions for the simplest ionic model fluid, the restricted primitive model, in Section 5. A brief comparative discussion of the results for the different simple and more complex fluids in Section 6 concludes the paper.

2. GENERAL METHODOLOGY

For all the different model fluids which are discussed in the following sections, the thermodynamic variables will be made dimensionless in terms of the energy and length scales characteristic of the respective model fluid. These will be the hard-core diameter σ and the energy of two particles at contact. Quantities that are reduced in this way will be denoted by starred symbols; the explicit expressions for the reduced temperature T^* and the density ρ^* will be given in the respective (sub)sections.

The functional of the interfacial free energy density within the square-gradient theory (an augmented van der Waals approach) that we used in all cases is

$$I[\rho^*] = \int_{-\infty}^{\infty} \left[\Delta\omega(\rho^*) + \frac{1}{2} T^* c(\rho^*) \left(\frac{\partial \rho^*}{\partial z^*} \right)^2 \right] \mathrm{d}z^*, \tag{2}$$

which, after minimization with respect to the density profile $\rho^*(z^*)$, yields the surface tension. The z^*-axis has been chosen to be perpendicular to the planar liquid–vapor interface. The quantity $\Delta\omega(\rho^*)$ is defined by $\Delta\omega(\rho^*) = \omega(\rho^*) + P^*_{\mathrm{bulk}}$, where P^*_{bulk} is the reduced bulk pressure in the coexisting phases and $\omega(\rho^*) = T^*(\phi_{\mathrm{hom}} - \rho^* \bar{\mu}_{\mathrm{bulk}})$, with $\bar{\mu}_{\mathrm{bulk}} = \beta \mu_{\mathrm{bulk}}$ being the reduced chemical potential and $\beta = (kT)^{-1}$. $\phi_{\mathrm{hom}} = \beta A_{\mathrm{hom}} \sigma^3 / V$, where V is the volume, denotes the reduced Helmholtz free energy density of a homogeneous system, i.e., one without an interface. The coefficient of the square-gradient term c is obtained from the correlation functions following from the respective level of theory used to describe the behavior of the model fluid [3–6].

Using the Euler–Lagrange equation, we may rewrite Eq. (2) as

$$\gamma^* = \int_{\rho_v^*}^{\rho_l^*} \sqrt{2T^* c(\rho^*)\Delta\omega(\rho^*)}\,\mathrm{d}\rho^*, \tag{3}$$

which allows one to calculate the surface tension directly without prior knowledge of the density profile [7]; here, γ^* denotes the reduced surface tension.

3. SIMPLE FLUIDS

We first consider simple fluids, the interaction potentials of which are spherically symmetric. Both the Yukawa fluid and the square-well fluid allow one to vary the range of the interaction potential systematically and to study the dependence of the corresponding-states surface tension on this parameter. The difference between the two fluids is the way in which the potentials decay to zero with increasing interparticle distance r.

3.1. Yukawa Fluid

For this model fluid, the interaction potential between two particles is defined by

$$u = \begin{cases} -\epsilon \dfrac{\exp[-\lambda(r-\sigma)/\sigma]}{r/\sigma} & r \geq \sigma \\ \infty & r < \sigma, \end{cases} \tag{4}$$

where ϵ is the depth of the potential and σ is the hard-sphere diameter. The range of the potential is tuned by varying λ. The reduced variables are $T^* = kT/\epsilon$, $\rho^* = \rho\sigma^3$, $P^* = P\sigma^3/\epsilon$, and $\gamma^* = \gamma\sigma^2/\epsilon$. For the calculations presented here, the excess part of the homogeneous free energy density ϕ^{ex} is approximated at the level of the second virial coefficient (2VC), $\phi^{\mathrm{ex}} = B^*\rho^{*2}$:

$$B^* = B/\sigma^3 = \frac{2\pi}{3} - 2\pi \sum_{n=1}^{\infty} \frac{1}{n!} \frac{\exp(n\lambda)}{T^{*n}} (n\lambda)^{n-3} \Gamma(3-n, n\lambda), \tag{5}$$

where Γ is the incomplete gamma function. To obtain ϕ_{hom}, we add the ideal-gas term and the Carnahan-Starling expression for the hard-sphere part (as a matter of course, the hard-sphere contribution to B^*, $2\pi/3$, is

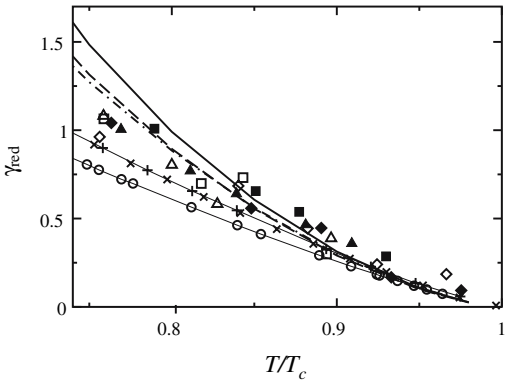

Fig. 1. Corresponding-states surface tension of the Yukawa fluid for different values of the inverse interaction-range parameter λ. Simulation data obtained from Monte Carlo simulations are given for $\lambda = 1.8$ (filled diamonds [8]), $\lambda = 3.0$ (filled triangles [9]), and $\lambda = 4.0$ (filled squares [9]), along with data from molecular-dynamics simulations [8] for $\lambda = 1.8$ (open diamonds), $\lambda = 3.0$ (open triangles), and $\lambda = 4.0$ (open squares). The thick lines are results from the 2VC theory: $\lambda = 1.8$ (dashed-dotted), $\lambda = 3.0$ (dashed), $\lambda = 4.0$ (continuous). The master curve for simple fluids is represented by the experimental data for $CHClF_2$ (plus) and $CHCl_2F$ (cross); the open circles are corresponding data for methane. The thin lines connecting the experimental data are meant to guide the eye.

not counted twice). The coefficient of the square-gradient term is obtained on the same level of approximation and c is given by $c = B^*_{\nabla^2}/3$, with

$$B^*_{\nabla^2} = B_{\nabla^2}/\sigma^5 = -\frac{2\pi}{5} + 2\pi \sum_{n=1}^{\infty} \frac{1}{n!} \frac{\exp(n\lambda)}{T^{*n}} (n\lambda)^{n-5} \Gamma(5-n, n\lambda). \qquad (6)$$

The results of the 2VC theory for the inverse interaction-range parameters $\lambda = 1.8$ (dashed-dotted), $\lambda = 3.0$ (dashed), and $\lambda = 4.0$ (continuous) are shown in Fig. 1 and compared to the corresponding simulation results of González-Melchor et al. [8] and of López-Rendón et al. [9] for this fluid (diamonds, triangles, and squares, respectively, where the filled symbols represent data from Monte Carlo simulations, while the open ones are results of molecular-dynamics simulations). The master curve for simple and weakly polar fluids is represented by $CHCl_2F$ (cross) and $CHClF_2$ (plus) [10] in this figure; the slightly deviating data for methane (circles)

[10], for which quantum effects play a role, are also given for comparison. It is seen that in the temperature range $0.9 \leq T/T_c \leqslant 1$, the theoretical results coincide with the master curve; for lower temperatures, one observes positive deviations from the master curve, which are more pronounced the *shorter* the interaction range, i.e., the larger λ. We will return to this interesting and maybe somewhat unexpected result in the next subsection. The simulation results [8,9] are found slightly above the master curve and lie between the master curve and the theoretical results for the temperature range $0.7 \leq T/T_c \leq 0.85$. While no clear trend of the influence of the inverse interaction-range parameter λ on the corresponding-states surface tension γ_{red} can be deduced from the earlier and somewhat noisy simulation data of González-Melchor et al. [8], the more recent and smoother data of López-Rendón et al. [9] seem to support the theoretical result that γ_{red} at a given reduced temperature T/T_c increases with increasing λ, i.e., with a decrease of the interaction range. A more extensive set of simulation data covering a wider range of values of λ is desirable to corroborate the observed trend.

3.2. Square-Well Fluid

The interaction potential of this fluid is particularly simple to handle analytically because, in each of the three regions, there is no explicit dependence on the interparticle distance r. The potential is defined by

$$u = \begin{cases} \infty, & r < \sigma \\ -\epsilon, & \sigma \leqslant r < l\sigma \\ 0, & r \geqslant l\sigma, \end{cases} \tag{7}$$

where σ is the diameter of a hard-sphere particle, ϵ is the well depth, and l is the range of the attractive interaction. All variables are made dimensionless as described in Section 3.1.

Although it is no problem to develop a theory at the level of the third virial coefficient [6], we restrict ourselves to the second virial (2VC) coefficient here in order to be able to compare to the results obtained for the Yukawa fluid on the same level. The corresponding expressions for B and B_{∇^2} are given in Ref. [6].

The results for the square-well fluid with interaction-range parameters $l = 1.5$ (continuous), $l = 2.0$ (dashed), and $l = 3.0$ (dashed-dotted) are shown in Fig. 2, where they are compared to simulation results [6,11] (filled symbols). As for the Yukawa fluid, the theoretical results as well as the simulation data coincide with the master curve (plus and cross) for $0.9 \leq T/T_c \leq 1$. The behavior at lower reduced temperature is more diverse

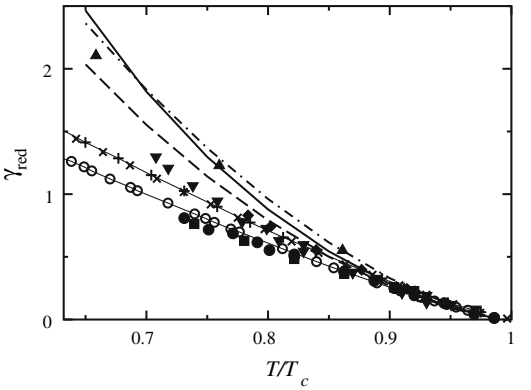

Fig. 2. Corresponding-states surface tension of the square-well fluid for different interaction-range parameters l. Simulation data are given for $l = 1.5$ (filled squares [6], filled circles [11]), for $l = 2.0$ (filled diamonds [6], filled triangles down [11]), and for $l = 3.0$ (filled triangles up [6]). The thick lines are results from the 2VC theory: $l = 1.5$ (continuous), $l = 2.0$ (dashed), $l = 3.0$ (dashed-dotted). The master curve for simple fluids is represented by the experimental data for $CHClF_2$ (plus) and $CHCl_2F$ (cross); the open circles are corresponding data for methane. The thin lines connecting the experimental data are meant to guide the eye.

and deserves a detailed discussion. For the shortest interaction range, $l = 1.5$, the simulation data lie below the master curve and seem to match the slightly anomalous behavior of methane (open circles) quite well. For the intermediate interaction range of $l = 2.0$, the simulation data show small positive deviations from the master curve for $T/T_c \leq 0.8$. The data for the longest interaction range, $l = 3.0$ [6], deviate significantly towards higher values of γ_{red}, so, from the simulations, there is clear evidence for the tendency of the corresponding-states surface tension to *increase* with increasing interaction range. This is exactly opposite to the theoretical predictions for the Yukawa fluid mentioned above. The results of the 2VC theory for the square-well fluid are inconclusive; apart from the temperature range $T/T_c < 0.7$, the data for $l = 1.5$ lie between the ones for $l = 2.0$, which are lowest, and the ones for $l = 3.0$, which describe the simulation data for this interaction range reasonably well. Interestingly, a theory based on the high-temperature limit of the second virial coefficient (denoted by "2HT" in Ref. 6), which may be referred to as a van der Waals theory, brings out the trend of increasing γ_{red} with longer interaction range correctly [6].

4. DIPOLAR FLUIDS

The simplest (and crudest) model of polar fluids is the system consisting of dipolar hard spheres (DHS). Within this model, the interaction potential between two particles i and k is given by

$$u_{ik} = \begin{cases} -\dfrac{m^2}{\epsilon_0 r_{ik}^3} D_{ik} & r_{ik} \geq \sigma \\ \infty & r_{ik} < \sigma, \end{cases} \tag{8}$$

where m is the dipole moment and $D_{ik} = 3\left(\hat{m}_i \cdot \hat{r}_{ik}\right)\left(\hat{r}_{ik} \cdot \hat{m}_k\right) - \hat{m}_i \cdot \hat{m}_k$ describes the angular dependence of the potential, r_{ik} is the distance between particles i and k, and the circumflexes denote unit vectors. ϵ_0 is the permittivity of vacuum. The reduced variables are defined as $T^* = kT\epsilon_0\sigma^3/m^2$, $\rho^* = \rho\sigma^3$, $P^* = P\epsilon_0\sigma^6/m^2$, and $\gamma^* = \gamma\epsilon_0\sigma^5/m^2$.

In real fluids consisting of polar molecules, there is always an additional contribution to the interaction potential from isotropic dispersion interactions, which result from the polarizability of the molecules. The limiting case of zero polarizability is, therefore, somewhat artificial, and it is still subject to discussion if the DHS system displays liquid–vapor coexistence and whether it has a corresponding critical point [12,13]. The simulations of van Leeuwen and Smit [12] suggested that a minimum strength of isotropic dispersion interactions is needed to observe liquid–vapor coexistence. Accordingly, no simulation results for the surface tension of the DHS fluid are available. Analytical theories for the DHS system, however, yield liquid–vapor coexistence [14]; we will compare the results obtained from Onsager theory [15], in conjunction with an approximate hypernetted chain (AHNC) relation to compute the square-gradient coefficient c [3], to the ones for real fluids.

Figure 3 shows the data for real polar fluids and the results obtained within the AHNC-Onsager theory (continuous). Once more, the master curve for simple and weakly polar fluids is represented by $CHClF_2$ (plus) and $CHCl_2F$ (cross)—many other polar fluids show the same corresponding-states behavior [3]. Deviations from this master curve are only found for strongly polar fluids, such as acetone (diamonds), and for polar fluids that tend to associate due to hydrogen bonding; prominent examples are compiled in the plot, namely, water (open circles), ethanol (triangles), methanol (open squares), and hydrogen fluoride (HF; filled circles [16] and filled squares [17]). These associating fluids display a sigmoid behavior of the surface tension as a function of temperature, which leads to lower values of γ_{red} for $T/T_c \leq 0.8$ as compared to the master curve. Truly anomalous is the behavior of HF, whose γ_{red} data remain significantly below the master curve for all temperatures [3,18].

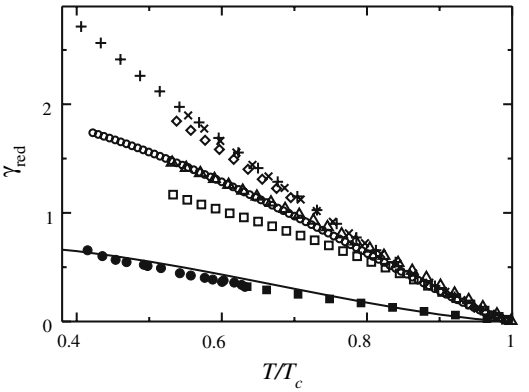

Fig. 3. Corresponding-states surface tension of polar fluids. $CHClF_2$ (plus) and $CHCl_2F$ (cross) define the master curve for simple and weakly polar fluids; deviations from this curve, in order of increasing extent, occur for acetone (diamonds), water (open circles), ethanol (triangles), methanol (open squares), and hydrogen fluoride (filled circles [16] and filled squares [17]). The continuous line represents results from the AHNC-Onsager theory.

Interestingly, HF is also the molecule which comes closest to the model of dipolar hard spheres due to its nearly spherical shape, the relatively large dipole moment, and an exceptionally small polarizability volume. It is therefore remarkable, but maybe not entirely surprising that the results for the AHNC-Onsager theory are anomalous, too, and nearly coincide with the HF data over the entire temperature range $0.4 \leq T/T_c \leq 0.95$. Another notable feature of the AHNC-Onsager theory is the occurrence of an inflection point in the graph of $\gamma_{red}(T/T_c)$ because association of the dipolar particles is not explicitly built into the theory [3].

5. IONIC FLUIDS

The simplest model of ionic fluids is the restricted primitive model (RPM), which consists of charged hard spheres of equal diameter, half of which carry a positive charge q, the other half a negative one. Within this model, the pair interaction between two particles i and k is defined by

$$u_{ik} = \begin{cases} \dfrac{q_i q_k}{\epsilon_0 r_{ik}} & r_{ik} \geq \sigma \\ \infty & r_{ik} < \sigma. \end{cases} \tag{9}$$

The permittivity ϵ_0 provides a structureless dielectric background (vacuum). The reduced variables are defined as $T^* = kT\epsilon_0\sigma/q^2$, $\rho^* = \rho\sigma^3$, $P^* = P\epsilon_0\sigma^4/q^2$, and $\gamma^* = \gamma\epsilon_0\sigma^3/q^2$.

Different theories have been developed to account for the properties of the RPM, the most famous one being the Debye–Hückel (DH) theory. Integral equation theories were devised, most notably the mean-spherical approximation (MSA), its generalized version (GMSA), and the hypernetted chain (HNC) closure. The former two have the advantage of yielding analytical expressions and a proper liquid–vapor coexistence curve, whereas the generally more accurate HNC closure fails to have solutions near the coexistence curve. All MSA-based theories predict a critical temperature that is considerably higher than the one found in simulations of the RPM. Currently, the most successful theory is the Fisher–Levin (FL) theory, an extension of the original DH theory, which accounts for ion pairing and interactions between ion pairs and free ions [19]. For this most promising theory, we employed an AHNC closure to calculate the square-gradient term [5]; Table I gives a largely extended set of data compared to the one we published earlier [5].

Table I. Coexistence Data (Temperature T^*, Vapor Density ρ_v^*, Liquid Density ρ_l^*) and Liquid–Vapor Interfacial Tension γ^* of the RPM within the AHNC-FL Theory

T^*	ρ_v^*	ρ_l^*	γ^*
0.040	0.00509283	0.767564	3.62×10^{-3}
0.041	0.00585088	0.669244	3.16×10^{-3}
0.042	0.00645620	0.582451	2.74×10^{-3}
0.043	0.00692623	0.505701	2.35×10^{-3}
0.044	0.00773890	0.440274	2.04×10^{-3}
0.045	0.00822085	0.381309	1.73×10^{-3}
0.046	0.00874028	0.329788	1.45×10^{-3}
0.047	0.00927285	0.284672	1.21×10^{-3}
0.048	0.00982078	0.245162	9.97×10^{-4}
0.049	0.0103632	0.210396	8.08×10^{-4}
0.050	0.0108846	0.179600	6.37×10^{-4}
0.051	0.0114864	0.152736	4.94×10^{-4}
0.052	0.0121206	0.128875	3.68×10^{-4}
0.053	0.0128673	0.107796	2.63×10^{-4}
0.054	0.0137588	0.0888564	1.72×10^{-4}
0.055	0.0149610	0.0717546	9.88×10^{-5}
0.056	0.0168152	0.0558765	4.32×10^{-5}
0.057	0.0207498	0.0396104	6.94×10^{-6}

The data are given in terms of reduced variables as defined in the main text.

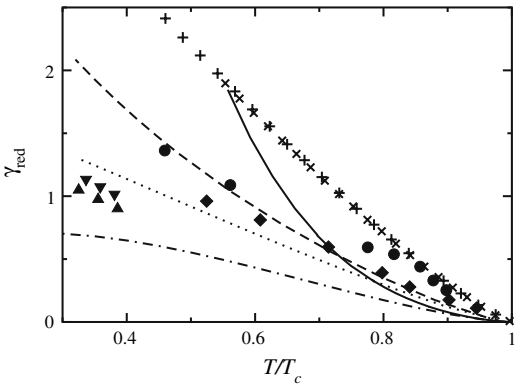

Fig. 4. Corresponding-states surface tension of ionic fluids. Experimental data for NaCl (triangles up) and for KCl (triangles down) are given along with results from simulations of the RPM (filled circles [21]) and of the SPM (diamonds [22]). The lines are theoretical results for the AHNC-FL (continuous), DH (dashed) and DH-CS (dotted) theories. For reference, the master curve for simple and weakly polar fluids is given by the representative substances $CHClF_2$ (plus) and $CHCl_2F$ (cross); furthermore, the data for the AHNC-Onsager theory are included for comparison (dashed-dotted line).

Experimental data for molten salts are relatively rare; the available ones are usually taken at temperatures that are far away from the critical point, which for salts may be located well above 3000 K [20].

Only two simulation studies of the surface tension of the RPM and a related model of soft charged spheres of equal size—the "soft primitive model" (SPM), in which the hard core of the particles in the RPM is replaced by a soft repulsion—have been reported [21,22]. In Fig. 4, these data (diamonds and circles) are shown along with experimental data for NaCl (triangles up) and KCl (triangles down) [20]. It is seen that the data are below the master curve for simple and weakly polar fluids (plus and cross), but higher than those for HF and the AHNC-Onsager theory (dashed-dotted line). The simulation data also suggest the presence of an inflection point indicating an association phenomenon, possibly ion pairing at lower temperatures. Remarkably, the most successful theory in the corresponding-states plot is the standard DH theory (dashed line); including the Carnahan-Starling term for the hard-sphere contribution (DH-CS theory, dotted line) leads to lower, but still decent results. The AHNC-FL theory (continuous), which is the best—and, in fact, the

only useful—theory up to now in terms of the absolute model parameters (comparison not shown) is found to yield unreliable results for $0.7 \leq T/T_c$. This behavior was anticipated [5] as the FL theory largely overestimates the liquid density at lower temperatures. Interestingly, none of the theories shows an inflection point in $\gamma_{red}(T/T_c)$. The more complete theory developed by the present authors [23], which also accounts for dipolar interactions between ion pairs and which reduces to the Onsager theory in the limit of complete ion pairing, however, is expected to display an inflection point.

As mentioned above, the MSA-based theories do not yield a good description in terms of the absolute model variables, mainly due to the overestimation of T_c. On the corresponding-states scale, the GMSA theory [24] gives satisfactory results that are too high by about 25% (not shown), while the MSA results of Groh et al. [25] are too large by a factor of 2.7 (not shown), which is remarkably close to the factor $\sqrt{8}$ of overestimation that we anticipated [4, 5] in view of the inappropriate local-density approximation that Groh et al. [25] used.

6. CONCLUSION

We have analyzed the corresponding-states surface tension, as defined by Guggenheim, of simple fluids with variable interaction range as well as for polar and ionic fluids. While experimental data for simple and weakly polar fluids collapse nicely onto a single master curve, deviations towards lower values of γ_{red} are observed for strongly polar, hydrogen-bonding, and associating fluids and for molten salts.

For the simple fluids with variable interaction range—the Yukawa fluid and the square-well fluid—theory and simulation do not give a clear trend of whether γ_{red} increases or decreases with increasing range of the interaction. While the simulation results for the square-well fluid indicate that γ_{red} increases, the available corresponding data for the Yukawa fluid seem to suggest the opposite behavior. The admittedly simple theory for this fluid based on the second virial coefficient predicts that γ_{red} decreases with increasing interaction range. For the square-well fluid, a theory on the same level gives no unambiguous answer to the question, while a simple van der Waals theory supports the trend observed in the simulations [6]. More extensive and more accurate simulations of the Yukawa fluid are desirable.

For polar fluids, one finds that, for systems in which no hydrogen bonds are formed, it takes very large dipole moments for visible deviations from the master curve to occur. In the cases which deviate notably, the contributions of dipole moment and hydrogen bonds are difficult to

separate. In such systems, the association of particles leads to an inflection point of γ_{red}. A recent article by the present authors investigated the transition from a simple fluid to a strongly polar fluid by gradually changing the relative strengths of isotropic dispersion interactions and directional dipolar interactions [3], and it was observed that γ_{red} decreases nonmonotonically with increasing relative strength of the dipolar interactions. It would be interesting to see a simulation study of this crossover.

There are insufficient experimental data to judge whether the sigmoid behavior seen for strongly polar systems is also found for ionic fluids. The available simulation data for ionic model fluids seem to support the presence of an inflection point, while none of the standard theories (DH-based or MSA-based) predicts sigmoid behavior, which suggests that the association of particles is not yet accounted for correctly.

ACKNOWLEDGMENTS

We would like to thank José Alejandre, Fernando Bresme, and Yan Levin for helpful discussions and Pedro Orea for supplying us with the numerical values of the data shown in Fig. 4 of Ref. [9]. Financial support from the German Research Foundation (Deutsche Forschungsgemeinschaft) and the Universität Bremen is gratefully acknowledged.

REFERENCES

1. E. A. Guggenheim, *J. Chem. Phys.* **13:**253 (1945); see also *Proc. Phys. Soc. (London)* **85:**811 (1965).
2. See, e.g., T. L. Hill, *An Introduction to Statistical Thermodynamics* (Addison–Wesley, Reading, Massachusetts, 1960, reprint: Dover, Mineola, New York, 1986).
3. V. C. Weiss and W. Schröer, *J. Chem. Phys.* **122:**084705 (2005).
4. V. C. Weiss and W. Schröer, *J. Phys.: Condens. Matter* **10:**L705 (1998).
5. V. C. Weiss and W. Schröer, *J. Phys.: Condens. Matter* **12:**2637 (2000).
6. P. Orea, Y. Duda, V. C. Weiss, W. Schröer, and J. Alejandre, *J. Chem. Phys.* **120:**11754 (2004).
7. J. S. Rowlinson and B. Widom, *Molecular Theory of Capillarity* (Clarendon, Oxford, 1982).
8. M. González-Melchor, A. Trokhymchuk, and J. Alejandre, *J. Chem. Phys.* **115:**3862 (2001).
9. R. López-Rendón, Y. Reyes, and P. Orea, *J. Chem. Phys.* **125:**084508 (2006).
10. Ch. Wohlfarth and B. Wohlfarth, *Surface Tension of Pure Liquids and Binary Liquid Mixtures*, Landolt-Börnstein, Vol. IV/16, M. D. Lechner, ed. (Springer, Berlin, 1997).
11. J. K. Singh, D. A. Kofke, and J. R. Errington, *J. Chem. Phys.* **119:**3405 (2003).
12. M. E. van Leeuwen and B. Smit, *Phys. Rev. Lett.* **71:**3991 (1993).
13. J.-M. Caillol, *J. Chem. Phys.* **98:**9835 (1993); J. J. Weis and D. Levesque, *Phys. Rev. Lett.* **71:**2729 (1993); S. C. McGrother and G. Jackson, *Phys. Rev. Lett.* **76:**4183 (1996); J. C. Shelley, G. N. Patey, D. Levesque, and J. J. Weis, *Phys. Rev. E* **59:**3065 (1999);

Y. Levin, *Phys. Rev. Lett.* **83:**1159 (1999); Y. Levin, P. S. Kuhn, and M. C. Barbosa, *Physica A* **292:**129 (2001); P. J. Camp, J. C. Shelley, and G. N. Patey, *Phys. Rev. Lett.* **84:**115 (2000); P. J. Camp and G. N. Patey, *Phys. Rev. E* **62:**5403 (2000).
14. J. W. H. Sutherland, G. Nienhuis, and J. M. Deutch, *Mol. Phys.* **27:**721 (1974); G. S. Rushbrooke, G. Stell, and J. S. Høye, *Mol. Phys.* **26:**1199 (1973); C. Joslin and S. Goldman, *Mol. Phys.* **79:**499 (1993).
15. L. Onsager, *J. Am. Chem. Soc.* **58:**1486 (1936).
16. J. H. Simons and J. W. Bouknight, *J. Am. Chem. Soc.* **54:**129 (1932).
17. C. F. Beaton and G. F. Hewitt, *Physical Property Data for the Design Engineer* (Hemisphere, New York, 1989).
18. J. K. Singh and D. A. Kofke, *J. Chem. Phys.* **121:**9574 (2004).
19. Y. Levin and M. E. Fisher, *Physica A* **225:**164 (1996).
20. G. J. Janz, *J. Phys. Chem. Ref. Data* **9:**791 (1980); G. J. Janz, *Molten Salts Handbook* (Academic, New York, 1967).
21. M. González-Melchor, J. Alejandre, and F. Bresme, *Phys. Rev. Lett.* **90:**135506 (2003).
22. M. González-Melchor, F. Bresme, and J. Alejandre, *J. Chem. Phys.* **122:**104710 (2005).
23. V. C. Weiss and W. Schröer, *J. Chem. Phys.* **108:**7747 (1998).
24. M. M. Telo da Gama, R. Evans, and T. J. Sluckin, *Mol. Phys.* **41:**1355 (1980).
25. B. Groh, R. Evans, and S. Dietrich, *Phys. Rev. E* **57:**6944 (1998).